

ROME prep. 94/1042

SHEP prep. 93/94-31

The Gluon Propagator on a Large Volume, at $\beta = 6.0$.

P. Marenzoni^a, G. Martinelli^b, N. Stella^c

^a Dip. di Ingegneria dell'Informazione

Università di Parma, Viale delle Scienze, 43100 Parma, Italy

^b Dip. di Fisica, Università degli Studi di Roma "La Sapienza" and
INFN, Sezione di Roma, P.le A. Moro 2, 00185 Rome, Italy.

^c Physics Department, "The University", S09 5NH Highfield, Southampton, U.K.

Abstract

We present the results of a high statistics lattice study of the gluon propagator, in the Landau gauge, at $\beta = 6.0$. As suggested by previous studies, we find that, in momentum space, the propagator is well described by the expression $G(k^2) = [M^2 + Z \cdot k^2(k^2/\Lambda^2)^\eta]^{-1}$.

By comparing $G(k^2)$ on different volumes, we obtain a precise determination of the exponent $\eta = 0.532(12)$, and verify that M^2 does not vanish in the infinite volume limit. The behaviour of η and M^2 in the continuum limit is not known, and can only be studied by increasing the value of β .

Submitted to Nuclear Physics B

Introduction

One of the most interesting, yet unresolved, issues concerning Quantum Chromodynamics, as a theory of strong interactions, is the comprehension of the transition from the fundamental fields, appearing in the Lagrangian, to the physical particles, namely the hadrons. While color confinement and hadronization are believed to occur, no consistent derivation of this mechanism from first principles is yet available, although much effort has been put in this direction.

By studying the propagation and the interaction of the fundamental fields, appearing in the QCD Lagrangian, one attempts to gain some insight on the mechanism of confinement and hadronization, which are genuine non-perturbative effects. In this paper, we present the results of a non-perturbative study of the gluon propagator, in the Landau gauge, obtained from a high statistics lattice simulation.

The results of the present study, on a volume larger than in refs. [1, 2], confirm that the gluon propagator is well described by the functional form proposed in the references above:

$$G(k^2) = \left[M^2 + Z \cdot (k^2) \left(\frac{k^2}{\Lambda^2} \right)^\eta \right]^{-1}. \quad (1)$$

We obtain a more precise determination of the exponent, finding $\eta = 0.532(12)$ and show that the gluon propagator at zero momentum stays finite, as the infrared cut-off is removed.

In section 1, we review what is known from perturbation theory, and some results obtained by perturbative analyses. Particular attention is devoted to other lattice simulations, whose results can be compared directly with ours. In section 2, the definition of the correlation functions will be given, together with a description of the numerical implementation. Section 3 is dedicated to the discussion of systematic effects and lattice artefacts. We found important to discuss these aspects before giving the results, which are largely influenced by our control of systematic errors. Finally, in section 4, we present the new results and compare them with those of our previous study [1], trying to interpret common features and differences.

1 The gluon propagator in the literature

As is the case for gauge-dependent quantities, the gluon propagator can only be defined once that the gauge has been fixed. In the following, we will solely be concerned with the Landau gauge, which corresponds to fulfill the condition

$$\partial_\mu A_\mu^a(x) = 0, \quad a = 1, \dots, 8, \quad (2)$$

where $A_\mu^a(x)$ are the gauge fields, and a the color index.

The gluon propagator in this gauge has the form

$$D_{\mu\nu}(k) = -i \int d^4x \langle |T(A_\mu(x)A_\nu(0))| \rangle e^{ikx} = G(k^2) \left(g_{\mu\nu} - \frac{k_\mu k_\nu}{k^2} \right), \quad (3)$$

where $G(k^2) = -1/k^2$ at tree level. When leading order perturbative corrections are taken into account, $G(k^2)$ takes the form

$$G(k^2) = -\frac{1}{k^2(1 + \Pi(k^2))} \simeq -\frac{1}{(k^2)^{1+\eta}}, \quad (4)$$

with $\eta^{\text{pert}} = -\gamma_G g^2/4\pi$ and $\gamma_G = -3/13$. Therefore, at values of the coupling constant corresponding to $\beta = 6.0$, $g^2 \sim 1$, these corrections correspond to a minor change, at most 5%, to the tree level expression¹.

Perturbative corrections to $G(k^2)$ cannot therefore account for the higher power of k^2 which is necessary to give a confining potential, in the one gluon-exchange approximation.

An analytic non-perturbative approach to the problem is indeed very difficult. The most elegant and neatest way to attack the problem is perhaps to solve the Dyson-Schwinger equations w.r.t. the renormalized gluon two-point function $D_{\mu\nu}(k)$. The infinite set of differential equations should satisfy the Slavnov-Taylor identities in order to preserve gauge invariance. Being the equations non linear, different solutions are allowed [3]–[5], and their interpretation, already difficult, is made even more uncertain by the approximations that one has to make to render the problem feasible.

¹ To obtain this estimate we have not considered the running of the coupling constant.

In ref. [6] a procedure for deriving the gluon propagator in the Minimal Landau Gauge, is presented. Subsequently, Zwanziger confirmed [7] the solution of ref. [6] by repeating the calculation on the lattice. In ref. [1], we have shown that this expression fails to reproduce the lattice behaviour.

In ref. [8], the first exploratory study on the lattice was presented. They found that the effective energy is an increasing function of the time (see below for definition), that the gluon propagator violates the spectral decomposition and, in particular, cannot have the form (3) with $G(k^2) \sim 1/(k^2+m^2)$. Subsequently, the authors of ref. [9, 10] tried to account for such a behaviour either by including the possible contribution of unphysical particles, or considering the solution proposed in refs. [6, 7].

Lately, to interpret the results of the lattice simulations, a new functional form has been proposed [1, 2]:

$$G(k^2) = \left[M^2 + Z \cdot (k^2) \left(\frac{k^2}{\Lambda^2} \right)^\eta \right]^{-1}. \quad (5)$$

This expression tries to mimic the effect of an anomalous dimension for the gauge field, and keeps $G(k^2)$ finite. The latter is a necessary condition, due to the fact that the lattice possesses an intrinsic infrared cut-off.

According to [1] $\eta = 0.4 \div 0.6$, whereas the authors of [2] quote $\eta = 0.35$. The value of the dimensionful parameter M^2 is more controversial, and difficult to determine because it is very small, of the order of the infrared cut-off. It is not clear whether M^2 will vanish in the infinite volume limit.

Since there is no a priori theoretical prediction of the functional form (5), several further investigations are in order. Namely,

1. reduce the ultraviolet cut-off by increasing the value of β , and try to determine M^2 and η in the continuum limit;
2. verify if (5) contains any gauge-independent information. This can be investigated by studying the gluon propagator in different gauges.

In this paper, we address a different issue, that is the dependence of the parameters of equation (5) on the infrared cut-off. Anticipating some of the results, we have indications that the dimensionful parameter M^2 is not

merely a finite volume artefact, and it would keep a non-zero value in the infinite volume limit. Its fate in the continuum limit, i.e. as $\beta \rightarrow \infty$, is not known. The value of the anomalous dimension η , on the other hand, does not seem to be affected by the presence of the infrared regulator. A major question is the interpretation of a finite value of the gluon propagator, at zero momentum.

2 The gluon propagator on the lattice

In this section, we establish the notation and the main formulae, to be used in the following. We also give a brief description of the algorithms, i.e. the Monte Carlo procedure, used to generate statistically independent configurations, and the method which has been used to fix the Landau gauge. We conclude by reporting some information about the accuracy achieved by our gauge-fixing algorithm.

2.1 Notations

The gluon propagator is studied on the lattice by looking at the euclidean two-point correlation functions:

$$D_{\mu\nu}(x, y) = \text{Tr}\langle A_\mu(x)A_\nu(y)\rangle, \quad (6)$$

where $\mu, \nu = 1, \dots, 4$ and the trace is intended over color indices. The corresponding expression in momentum space is

$$D_{\mu\nu}(k) = G(k^2) \left(\delta_{\mu\nu} - \frac{k_\mu k_\nu}{k^2} \right). \quad (7)$$

Among the possible definitions of the gluon field on the lattice, we choose

$$A_\mu(x) = \frac{U_\mu(x) - U_\mu^\dagger(x)}{2i}. \quad (8)$$

In a previous publication [1], we have discussed in detail the motivations for such choice.

In order to study the gluon propagator in momentum space, $D_{\mu\nu}(k)$, we take the 4-dimensional Fourier transform of the correlators (6). Taking into account translation invariance, $D_{\mu\nu}$ is given by

$$D_{\mu\nu}(k) = \sum_{\vec{x}, t} \text{Tr} \langle A_\mu(x) A_\nu(0) \rangle e^{ikx}. \quad (9)$$

On the lattice, k can only take discrete values, $k_\mu = (2\pi/L_\mu a)n$, where a is the lattice spacing, and $n = 0, 1, \dots, L_\mu - 1$.

Moreover:

- we always take full advantage of space-time translational symmetry by averaging the previous expression over different points on the euclidean lattice;
- from r.h.s. of (9) the scalar function $G(k^2)$ is extracted, by taking suitable combinations of the spin indices μ, ν accordingly to (7).
- in order to check the validity of continuum dispersion relation on the lattice, the following four classes of correlators have been considered:

1. Transverse correlations

$$D_{ii}(k) = \sum_{\vec{x}, t} \text{Tr} \langle A_i(x) A_i(0) \rangle e^{ik_j x_j} e^{ik_0 t} = G(k^2) \delta_{ii}, \quad (10)$$

where $i, j = 1, \dots, 3$ and the spatial momentum k_j is non-zero only along axis orthogonal to the spin direction i .

2. Longitudinal correlations

$$D_{jj}(k) = \sum_{\vec{x}, t} \text{Tr} \langle A_j(x) A_j(0) \rangle e^{ik_j x_j} e^{ik_0 t} = G(k^2) \left(\delta_{jj} - \frac{k_j^2}{k^2} \right), \quad (11)$$

where $j = 1, \dots, 3$ and the spatial momentum has a non-zero component along the direction of the spin j .

3. Non-diagonal correlations

$$D_{ij}(k) = \sum_{\vec{x}, t} \text{Tr} \langle A_i(x) A_j(0) \rangle e^{i\vec{k} \cdot \vec{x}} e^{ik_0 t} = -G(k^2) \frac{k_i k_j}{k^2}, \quad (12)$$

where $i, j = 1, \dots, 3$ and $i \neq j$. These correlations do not vanish only when the spatial momentum is non-zero along both i and j directions.

4. Temporal correlations

$$D_{00}(k) = \sum_{\vec{x}, t} \text{Tr} \langle A_0(x) A_0(0) \rangle e^{i\vec{k} \cdot \vec{x}} e^{ik_0 t} = G(k^2) \left(\delta_{00} - \frac{k_0^2}{k^2} \right). \quad (13)$$

Further investigations of the behaviour of the gluon propagator can be carried on by looking at some correlations, which are functions of the spatial momentum and euclidean time. For simplicity we maintain the same notation given before, namely, we will consider:

1. Transverse correlations

$$D_{ii}(t, \vec{k}) = \sum_{\vec{x}} \text{Tr} \langle A_i(x) A_i(0) \rangle e^{ik_j x_j}, \quad (14)$$

2. Temporal correlations

$$D_{00}(t, \vec{k}) = \sum_{\vec{x}} \text{Tr} \langle A_0(x) A_0(0) \rangle e^{i\vec{k} \cdot \vec{x}}. \quad (15)$$

All the previous expressions have been computed for the following values of spatial momenta: $\vec{k} = (0, 0, 0)$, $(2\pi/24a, 0, 0)$, $(4\pi/24a, 0, 0)$, and $\vec{k} = (2\pi/24a, 2\pi/24a, 0)$. Moreover, permutations of the three spatial axes have been considered. The Fourier transform, with respect to the time coordinate has been computed allowing k_0 to take all the possible values. Namely, $k_0 = (2\pi/48a)n$, with $n = 0, \dots, 47$.

2.2 Lattice setup and gauge-fixing

We summarize the parameters of the present simulation in tab. 1. The only differences, with respect to ref. [1], are the lattice size and the number of configurations. All the others parameters of the simulation have been left unchanged, with the purpose of studying the dependence of expression (5) on each of them. For the generation of the pure gauge fields we adopted a Hybrid

	β	# confs.	Volume	$\partial_\mu A_\mu$
present work	6.0	500	$24^3 \times 48$	$< 10^{-6}$
ref. [1]	6.0	1000	$16^3 \times 32$	$< 10^{-6}$

Table 1: Summary of the parameters of the present simulation and of those of the simulation of ref. [1]

Monte Carlo (HMC) algorithm in its local version and with a checkerboard update, as described in [11]. This version of the HMC allows very short autocorrelation times among pure gauge configurations and is very effective when high statistic measures are needed. In our simulation we performed an initial thermalisation of 1024 iterations and then we extracted configurations every 128 iterations.

A further comment on the size of the statistical sample: although the number of configurations generated during the present run, is a half the old one, we have obtained more accurate results. This is due to the fact that the larger number of lattice points (the ratio of the two volumes is about 8) improves the stability of the signal.

In presence of gauge-dependent quantities, the accuracy of the gauge-fixing algorithm is a crucial information. Uncertainties in the gauge-fixing result in residual fluctuations, thus causing extra noise and/or systematic alterations. For this reason, the accuracy can only be established by performing tests on the gauge-dependent operators under study.

As demonstrated in ref. [1], the residual fluctuation left-over after gauge-fixing

$$\langle \partial_\mu A_\mu(x) \rangle_{\text{Latt}} \leq 10^{-6}, \quad (16)$$

are absolutely negligible, with respect to the statistical errors. Since we consider this to be a crucial point, we have repeated the same analysis as in [1] on the new sample. We have defined logarithmic (symmetric) derivatives, with respect to t , of transverse and temporal correlators, at zero spatial momentum. As in ref. [1], we find that the temporal correlator is constant and its derivative always compatible with zero, within errors. This qualitative behaviour can be compared with a similar figure in ref. [9].

t	$D_{00}(t, \vec{0})$	t	$D_{00}(t, \vec{0})$	t	$D_{00}(t, \vec{0})$
1	56552	6	56547	11	56545
2	56552	7	56549	12	56547
3	56550	8	56548	13	56542
4	56549	9	56547	14	56543
5	56548	10	56548	15	56543

Table 2: $D_{00}(t, \vec{0})$, measured on one configuration, as a function of the time separation. The gluon field $A_0(t, \vec{k})$ is constant in time, as required by the gauge condition.

A different check can be performed by noting that the condition (2) implies that the three dimensional Fourier transform of the gauge field $A_0(t, \vec{k} = \vec{0})$ is time independent. This time independence should hold on each single configuration. This has been checked by looking at the temporal correlation $D_{00}(t, \vec{0})$ of some arbitrarily chosen configurations. In table 2, we report the value of $D_{00}(t, \vec{0})$, at different time separations, on a single configuration. $D_{00}(t, \vec{0})$ is constant at the level of 0.008%, which is in fact consistent with the precision (16). Results in table 2 are to be compared with figure 1 of ref. [2], where the gluon field, plotted versus t after gauge-fixing, shows a strong time dependence.

The previous discussion shows that the present gauge-fixing procedure is the most effective one, among those implemented in the literature.

3 Results for the gluon propagator

In this section, we outline the unusual behaviour of the effective energy. Then, we consider the dependence of $G(k^2)$ on the momentum. Assuming the validity of the functional form (5), we first discuss in length systematic effects, and give our final results.

3.1 The behaviour of the effective energy

Using spectral decomposition and translation invariance, the correlation functions can be rewritten as

$$D(t, \vec{k}) = \sum_{|i\rangle} \frac{|\langle A(0)|i\rangle|^2}{\mathcal{N}_i} e^{-E_i t}, \quad (17)$$

where the sum is intended over all the states with the quantum numbers of operator $A(x)$ and $E_i = \sqrt{m_i^2 + |\vec{k}|^2}$ is the energy of the state i . The normalization \mathcal{N}_i is positive for physical states. From eq. (17), the effective energy

$$\omega_{\text{eff}}(t, \vec{k}) = \log \frac{D(t, \vec{k})}{D(t+1, \vec{k})}. \quad (18)$$

should be a decreasing function of the time, for any value of the momentum \vec{k} .

In figure 1, we report $\omega_{\text{eff}}(t, \vec{k})$ computed from the transverse correlators (14). $\omega_{\text{eff}}(t, \vec{k})$ is clearly increasing with time, for all the momentum combinations considered. Some authors [9] tried to justify this result by including (17) the contribution of unphysical particles, whose normalization is negative. The function apt to fit the lattice points, at large time separations, would then be:

$$F(t) = \frac{Z_1}{2m_1} e^{-m_1 t} + \frac{Z_2}{2m_2} e^{-m_2 t}; \quad Z_1 < 0, Z_2 > 0; \quad m_1 > m_2. \quad (19)$$

In our previous paper [1], we showed that (19) fails to reproduce the behaviour of $D_{\mu\nu}(t, \vec{k})$. The apparent agreement of (19) with $D(t, \vec{k} = \vec{0})$ in ref. [9], was probably faked by the large statistical errors.

3.2 Systematic effects

The systematic effects discussed in the following are those due to the infrared and ultraviolet cut-offs, introduced when the theory is regularized on a finite lattice. These effects limit the range of momenta, where reliable results can be obtained. A way to detect such effects is to look for discrepancies between

continuum dispersion relations and their lattice realization. We note that, contrary to what happens for other quantities, the quenched approximation is not going to produce systematic changes, being the pure gauge sector a self-consistent part of the theory. One then expects these results to stay valid *per se*, as a description of the pure gauge behaviour, although they might differ in the full theory. Another source of systematic uncertainty is the value of lattice spacing, which is found to vary substantially depending on the physical observable used to fix it. We will only be concerned about this point at the end of this section, when we will express, in physical unit, the propagator at zero momentum.

We discuss the effects of the ultraviolet cut-off, first. It is known that the presence of a finite ultraviolet cut-off produces unwanted effects, when momenta are of the order of the cut-off itself. On the lattice, this means that results, corresponding at momenta such that $k^2 a^2 > 1$, contain discretization contributions. A demonstration of the above statement, is given in figure 2A, where $G(k^2)$ is plotted as a function of k^2 in dimensionless units. In correspondence of the same value of k^2 , $G(k^2)$ can have different values, due to the breaking of the Lorentz symmetry. The different results correspond to $G(k^2)$, as extracted from the four classes of correlators (10)–(13). They agree within errors until $k^2 a^2 \simeq 1$ where they start clustering into two separated curves. This behaviour, at larger momenta, is caused by the fact that, in the Fourier transforms (10)–(13), we only increase k_0 , to the larger values allowed on the lattice, while $k_i, i = 1, 2, 3$ are always kept small. Points lying on the higher curve are those generated through spatial correlators (10)–(12), while, on the lower curve, there are the points computed from the temporal correlators (13), which are directly proportional to k_0^2 and so more affected by discretization effects, at large k_0 .

To verify this hypothesis, we have tried a kinematical correction to the momentum, substituting

$$\begin{aligned}
 k_\mu &\longrightarrow \mathcal{K}_\mu = 2 \sin\left(\frac{k_\mu}{2a}\right), \\
 k^2 &\longrightarrow \mathcal{K}^2 = \sum_{\mu=1}^4 \left(2 \sin\left(\frac{k_\mu}{2a}\right)\right)^2
 \end{aligned}
 \tag{20}$$

in the dispersion relation (7). Such a correction is suggested by the tree level expression of the bosonic propagator on the lattice. In fig. 2B, $G(k^2)$,

obtained by performing the substitutions (20), is shown. One sees that the two curves of fig. 2A have collapsed into a single one. On a logarithmic scale, the curve, obtained by using (20) appears as a straight line, at large k^2 , whose slope is the exponent $1 + \eta$ of equation (5). Around $\mathcal{K}^2 a^2 = 1$ the curve changes slope and η is slightly reduced. We cannot tell whether this behaviour is due to residual cut-off effects, or to the fact that, as the momentum increases, η is going towards its perturbative value. This issue can only be decided by decreasing the lattice spacing, i.e. by going to larger values of β , and increasing the range of k^2 , where lattice artefacts are small and momenta are large in physical units.

The investigation of the effects of the infrared cut-off is delicate and is directly related to the determination of the value of M^2 in (5). At very low momenta, different determinations of $G(k^2)$ corresponding to the same value of k^2 are inconsistent (see fig. 3). This effect is due to the fact that our lattice has different length, along the spatial and temporal axes. In fig. 3, we indicate, with an arrow, the value of k^2 where the differences became negligible.

We deduce from the previous analysis that one should only take into consideration the region of intermediate momenta. More quantitative indications in this sense are provided the fitting procedure, see below.

3.3 Fitting procedure

In the previous section, it has been shown that infrared and ultraviolet effects are reasonably small, only in the intermediate region of momenta. On large volumes, the region of momenta “free” from cut-off effects contains many points, which can be used to check the stability of the fits. The fitting function is the dimensionless version of (5)

$$G(k^2) = \frac{1}{M_L^2 + Z_L(k^2)^{1+\eta}}, \quad (21)$$

which depends on three free parameters. We fit first $G(k^2)$ to expression (21), on an interval of 6 points, which we move back and forth in the selected region of momenta. The fit is then repeated using the same procedure with 8 and 12 points, respectively. In the central region of k^2 , the results are

perfectly compatible on different k^2 -ranges and their stability improves, by increasing the number of points.

In figure 5, we plot the best 12-points fits for η and M^2 , together with the corresponding value of χ_{ndof}^2 , as a function of the minimum momentum considered in the fit (k_{min}^2). As anticipated in the previous section, for low and high momenta the fits are rather poor, giving unstable values for the parameters and a large χ_{ndof}^2 . At momenta $k_{\text{min}}^2 a^2 \simeq 0.1$ the values of χ_{ndof}^2 lower to $1 \div 1.5$ and the estimates for η and M^2 become very stable. Our final determination obtained by averaging over the four points indicated in the figure, is

$$\left\{ \begin{array}{l} M_L^2 = 4.46(9) \times 10^{-3} \\ Z_L = 0.102(1) \\ \eta = 0.532(12) \\ \langle \chi_{\text{ndof}}^2 \rangle = 1.08 \end{array} \right. \quad (22)$$

One can compare the present results with those of ref. [1]. We have re-analyzed the old result, by fitting $G_1(t)$ to expression (21)². On a volume $V = 16^3 \times 32$ we find:

$$\left\{ \begin{array}{l} M_L^2 = 2.8(1) \times 10^{-3} \\ Z_L = 9.01(4) \times 10^{-2} \\ \eta = 0.56(6) \\ \chi_{\text{ndof}}^2 = 1.5 \end{array} \right. \quad (23)$$

4 Discussion of the results

Apart from the value of M^2 (see next section), the agreement between the two sets of results is reasonably good, and the quality of the fits is satisfactory. By increasing the volume, we have obtained a more accurate estimate of the exponent η .

In our previous paper, we have quoted three different sets of results, obtained by studying different correlators, as functions of k^2 or \vec{k}, t respectively. We interpreted the differences as systematic effects. We are now able to check this interpretation. On a smaller volume, we had a limited choice

²In is necessary to change the overall normalization of $G_1(t)$, in order to make it independent on the lattice volume.

of momenta, before running into problems when $k^2 a^2 \simeq 1$ or infrared effects become important. As figure 3 shows, some of the points we had considered in ref. [1], in the fit of the propagator in momentum space, (see eq. (19) in ref. [1]), correspond to incompatible estimates of $G(k^2)$. For this reason, in ref. [1], the fit performed in momentum space, was giving results incompatible with those of eqs. (22) and (23), and it also disagrees with the present result (22).

In ref. [2], all the values of momenta, (including those corresponding to $k^2 a^2 \geq 1$) have been considered in the fit. Due to the flattening of the curve in the region of large momenta, the value of η has been underestimated.

Finally, we observe that the finite value of V has a very small effect in the determination of η , provided that the range of k^2 is large enough.

4.1 Comments on the value of M^2

The main difference between (22) and (23) is the value on the parameter M^2 , which increases with the volume. This observation rules out the hypothesis that the non-zero value found for M^2 is merely due to finite volume effects. If this were the case, we would expect M^2 to scale roughly as $1/L^2$.

Further arguments may be provided to reinforce the conclusion that $M^2 \neq 0$. In figure 3, values of $G(k^2)$ measured on a $16^3 \times 32$ lattice are over-imposed to the present data. We notice that $G(k^2 = 0)$, whose inverse gives an estimate of M^2 , is smaller on the largest volume. This is opposite to the expectation $M^2 \propto 1/L^2$.

A second argument is provided by the comparison of the fit to the data. In figure 4, the best fitting curve is compared to the lattice numbers, showing a good agreement even outside the fitting range. On the right side, the ratio data to fit shows that the fit overshoots the data, at low momenta. That is, the behaviour of the propagator at the so called intermediate momenta is consistent with a value of M^2 larger than $G(k^2 = 0)$ found on the lattice. This is a further proof that the effect of the infrared cut-off is to fake a value of M^2 lower than the real one.

It is possible to try a first, very crude extrapolation of the value of M^2

to the infinite volume limit. Using

$$M^2(V) = M^2(V = \infty) + \text{const} \frac{1}{\sqrt{V}}, \quad (24)$$

we get

$$M^2(V = \infty) = 6.202(8) \times 10^{-3}. \quad (25)$$

By using $a^{-1} \sim 2$ GeV, as it is determined by several lattice simulations at $\beta = 6.0$, this corresponds to

$$M_{\text{phys}}^2 \simeq (160 \text{ MeV})^2 \simeq (\Lambda_{QCD})^2 \quad (26)$$

It is fundamental to understand the behaviour of M^2 in the continuum, i.e. as $\beta \rightarrow \infty$. Notice that, even if M^2 stays finite in this limit, it cannot be interpreted as a symptom of symmetry breaking, since, in (5), M^2 does not represent a pole. An interpretation of this result, in connection with colour confinement is, at present, absent.

5 Conclusions

The study of the gluon propagator on different lattice volumes at fixed value of the coupling constant, confirms that $G(k^2)$ is well described by the expression (5). The value of the anomalous dimension η has been confirmed to assume a value slightly exceeding 0.5. By increasing the volume from $16^3 \times 32$ to $24^3 \times 48$, we have obtained a better determination of the anomalous dimension: $\eta = 0.532(12)$. We find that M^2 does not vanish as $1/L^2$. Assuming $a^{-1} \simeq 2$ GeV, our best estimate is $M_{\text{phys}}^2 \simeq (160\text{MeV})^2$.

Further investigations to study the continuum limit and the gauge-dependence of the results presented above are certainly required. If, ultimately, M^2 should stay finite, the comprehension of the mechanism which allows the gluon to develop a mass-scale in the infrared region would call for a theoretical understanding.

Acknowledgements

We are largely indebted to M. Testa for valuable discussions and for the support he gave to this project. We warmly thank the Thinking Machines Corporation for allowing us to exploit the considerable amount of CPU-time and of memory, needed for the present simulation. We are especially grateful to the staff of the “Centre National de Calcule Parallel en Sciences de la Terre” of Paris, for their precious help during all the stages of the simulation. We acknowledge the partial support of the M.U.R.S.T., Italy, and the European Union for partial support. N.S. wishes to thank the Noopolis-Sovena Foundation for financial support. G.M. and N.S. thank CERN, Geneva, for ospitality during the final stage of this work.

References

- [1] P.Marenzoni, G.Martinelli, N.Stella, M.Testa, *Phys. Lett.*, **B318**, (1993), 511.
- [2] C. Bernard, C. Parrinello, A. Soni, *Phys. Rev.* **D49** (1994) 1585.
- [3] N. Brown and M. Pennington. *Phys. Rev.*, **D38**, (1988), 2266.
- [4] N. Brown and M. Pennington. *Phys. Rev.*, **D39**, (1989), 2723.
- [5] M. Stingl. *Phys. Rev.*, **D34**, (1986), 3863.
- [6] V.N. Gribov. *Nucl. Phys.*, **B139**, (1978), 19.
- [7] D. Zwanziger. *Nucl. Phys.*, **B378**, (1992), 525.
- [8] J. E. Mandula and M. Ogilvie, *Phys. Lett.*, **B185**, (1987), 127.
- [9] R. Gupta *et al.* *Phys. Rev.*, **D36**, (1987), 2813.
- [10] C. Bernard, C. Parrinello and A. Soni, *Nucl. Phys.* **B (Proc. Suppl.) 30** (1992) 535.
- [11] . P. Marenzoni, G. Pugnetti and P. Rossi. *Phys. Lett.*, **B315** (1993) 152.
- [12] C.T.H. Davies. *Phys. Rev.*, **D37**, (1988), 1581.

$$\omega_{\text{eff}}(t, \vec{k})$$

t

Figure 1: Effective energy for transverse correlators (20). The effective energy is increasing with time for all the values of \vec{k} . The four curves correspond to the following momenta: \square : $\vec{k} = \vec{0}$, \diamond : $\vec{k} = (2\pi/24, 0, 0)$, \times : $\vec{k} = (2\pi/24, 2\pi/24, 0)$ and \circ : $\vec{k} = (4\pi/24, 0, 0)$

$G^{-1}(k^2)$

Figure A

Figure B

 $k^2[a^2]$ $\mathcal{K}^2[a^2]$

Figure 2: Behaviour of $G^{-1}(k^2)$ at high momenta. Fig. 2A: we observe the data splitting into two curves at high momenta ($k^2 a^2 \sim 1$). Fig. 2B: the two curves are mapped into a single line when the kinematical correction (26) is applied. The logarithmic behaviour of the corrected curve is much closer to a straight line.

$G(k^2)$

$$V = 16^3 \times 32$$

$$V = 24^3 \times 48$$



$k^2[a^2]$

Figure 3: Behaviour of $G(k^2)$ at low momenta. The arrow indicates the value of k^2 where different estimates of $G(k^2)$ start to agree, within the errors.

$$G^{-1}(k^2)$$

$$k^2[a^2]$$

$$k^2[a^2]$$

Figure 4: Best fit for the propagator in momentum space with the function (27). The figures show the fit (left) and the data to fit ratio, the dashed lines indicate the fitting range. The ratio shows that the fit overshoots the data for small momenta.

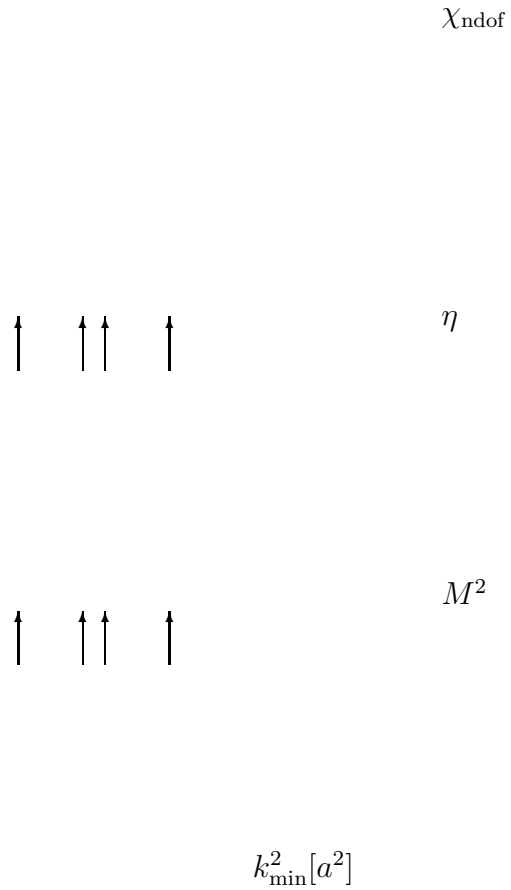
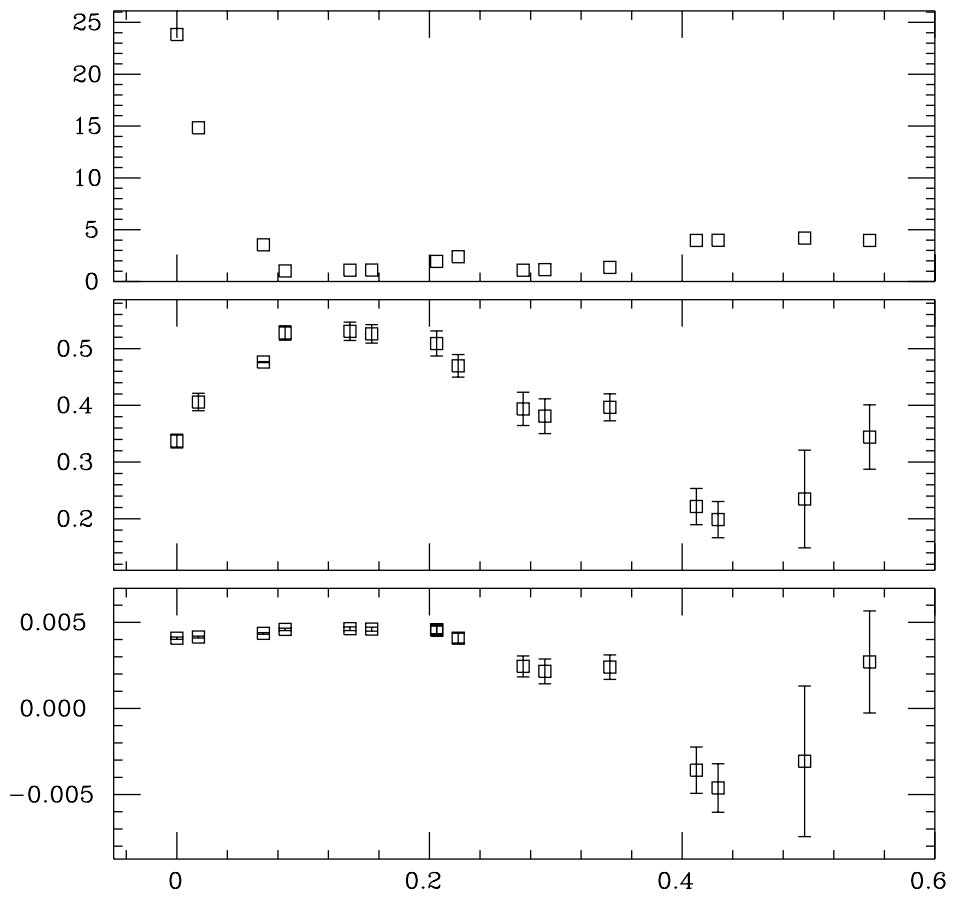
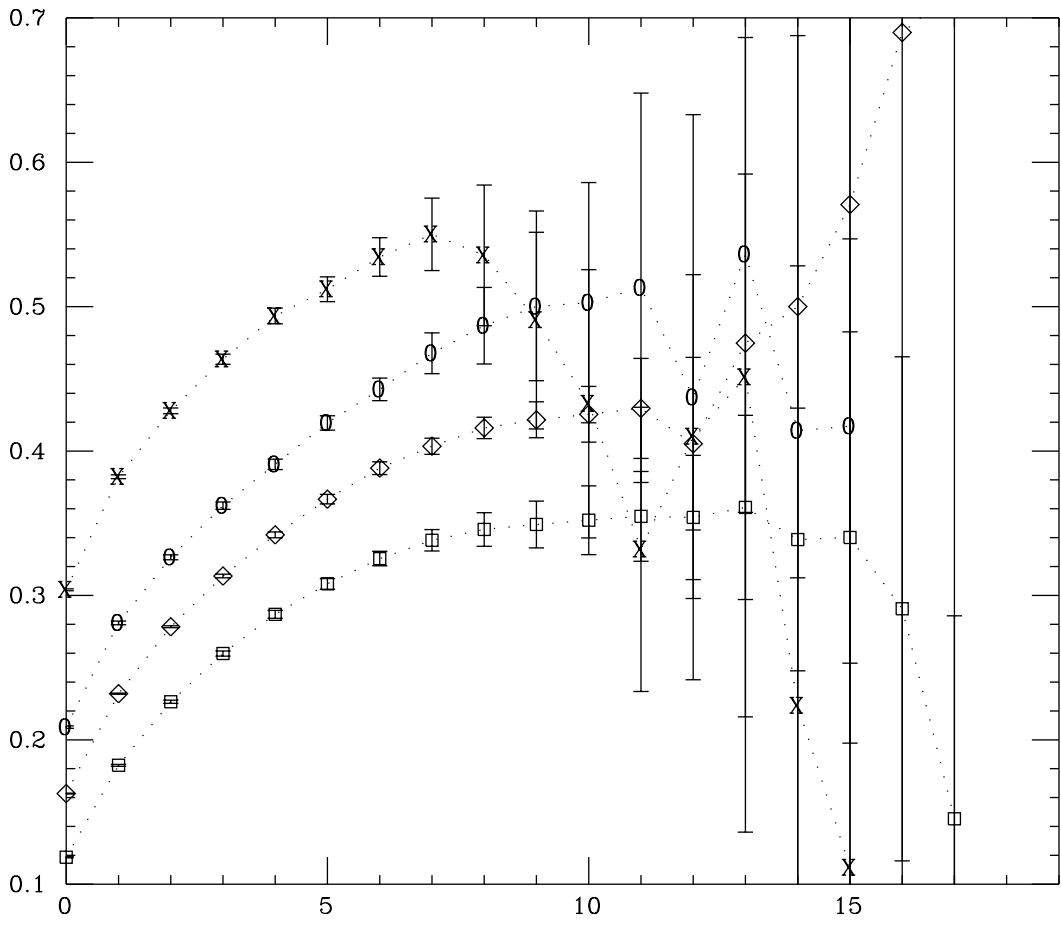


Figure 5: Values for M^2 and η versus the minimum momentum considered. The correspondent χ_{ndof}^2 is also shown. In this fit we considered 12 points.



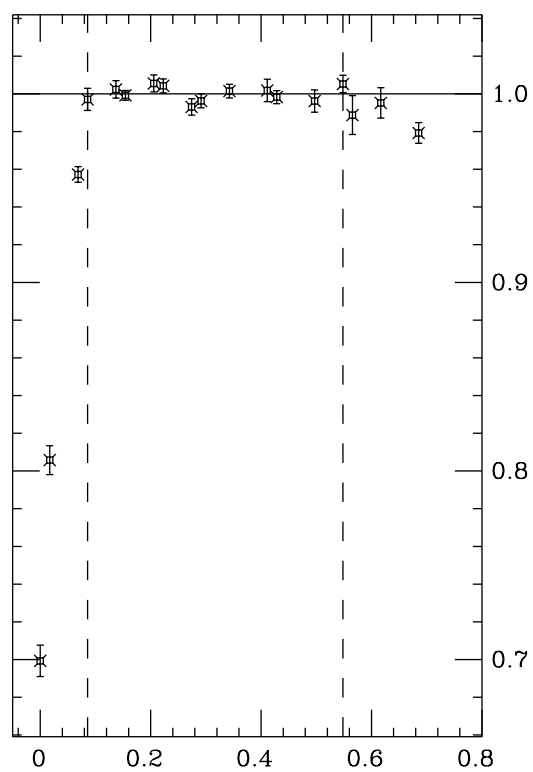
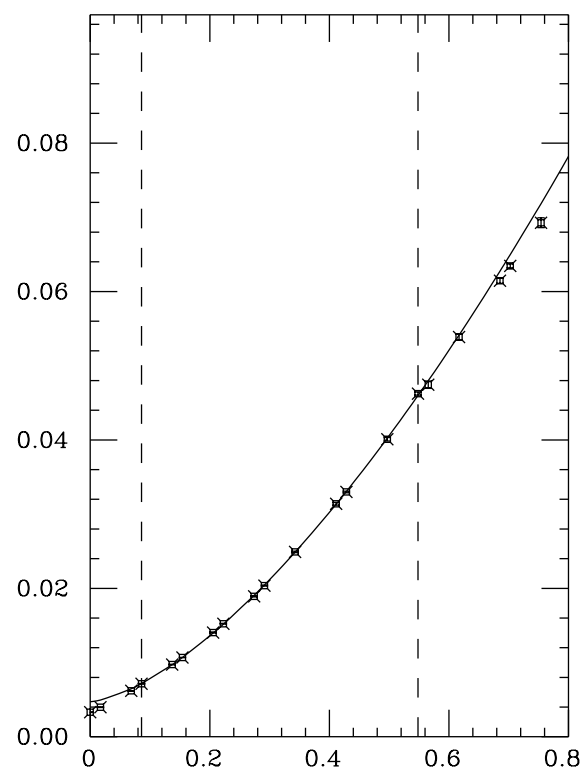


This figure "fig1-1.png" is available in "png" format from:

<http://arxiv.org/ps/hep-lat/9410011v2>

This figure "fig1-2.png" is available in "png" format from:

<http://arxiv.org/ps/hep-lat/9410011v2>



This figure "fig1-3.png" is available in "png" format from:

<http://arxiv.org/ps/hep-lat/9410011v2>

This figure "fig1-4.png" is available in "png" format from:

<http://arxiv.org/ps/hep-lat/9410011v2>

This figure "fig1-5.png" is available in "png" format from:

<http://arxiv.org/ps/hep-lat/9410011v2>

